



This is a repository copy of *Systematic design study into the influence of rotational speed on the torque density of surface-mounted permanent magnet machines*.

White Rose Research Online URL for this paper:  
<http://eprints.whiterose.ac.uk/151297/>

Version: Published Version

---

**Article:**

Yu, A. and Jewell, G.W. [orcid.org/0000-0002-8763-4190](https://orcid.org/0000-0002-8763-4190) (2019) Systematic design study into the influence of rotational speed on the torque density of surface-mounted permanent magnet machines. *The Journal of Engineering*, 2019 (17). pp. 4595-4600.

<https://doi.org/10.1049/joe.2018.8204>

---

**Reuse**

This article is distributed under the terms of the Creative Commons Attribution (CC BY) licence. This licence allows you to distribute, remix, tweak, and build upon the work, even commercially, as long as you credit the authors for the original work. More information and the full terms of the licence here:  
<https://creativecommons.org/licenses/>

**Takedown**

If you consider content in White Rose Research Online to be in breach of UK law, please notify us by emailing [eprints@whiterose.ac.uk](mailto:eprints@whiterose.ac.uk) including the URL of the record and the reason for the withdrawal request.



[eprints@whiterose.ac.uk](mailto:eprints@whiterose.ac.uk)  
<https://eprints.whiterose.ac.uk/>

# Systematic design study into the influence of rotational speed on the torque density of surface-mounted permanent magnet machines

eISSN 2051-3305  
Received on 26th June 2018  
Accepted on 30th July 2018  
E-First on 21st May 2019  
doi: 10.1049/joe.2018.8204  
www.ietdl.org

Anshan Yu<sup>1</sup>, Geraint W. Jewell<sup>1</sup> ✉

<sup>1</sup>Department of Electronic and Electrical Engineering, Rolls-Royce University Technology Centre in Advanced Electrical Machines, The University of Sheffield, 3 Solly Street, Sheffield. S1 4DE, UK

✉ E-mail: g.jewell@sheffield.ac.uk

**Abstract:** A series of systematic studies are carried out to investigate the influence on torque density and power density on machine speed rating. Several series of permanent magnet machine designs are established using an array of different electrical and thermal design constraints. The paper demonstrates that torque density in permanent magnet machines tends to decrease with speed rating due to complex interplay between electromagnetic and mechanical considerations, e.g. fixed winding current density, fixed split ratio etc. Interesting trends are observed, including cases in which there is an optimum rotational speed in terms of power density, beyond which the power density starts to decrease with increased speed rating.

## 1 Introduction

It is a well-established maxim of electrical machine design that machines are sized on the basis of their torque rating rather than their power rating per se. This in turn leads to the well-founded notion that power density increases with increasing rotational speed. However, it is also recognised that this is neither a linear relationship nor indeed necessarily a monotonic relationship as there are several speed-related features of performance that diminish the achievable torque density for a given set of constraints, e.g. the need to incorporate rotor magnet containment, stator core loss, rotor magnet loss and in some case, the power quality of the current waveform. There are several papers which have collated and reviewed design data from literature on different individual designs for high-speed applications [1–4]. In [1], the authors provide a curve fitting demonstrating a trend of torque density variation with machine operating speed. However, since the collated machine designs are aimed at different applications with differing constraints and limited consistency on whether the ratings are for steady-state continuous, this data collation approach, although illustrative of typical trends, does not provide a systematic and rigorously quantitative indication of the variation in torque density with machine speed rating.

This paper presents a systematic series of design studies which aims to establish the dependency between torque density and rotational speed within the specific context of a 250 kW rated permanent magnet machine with surface-mounted magnets.

## 2 Design methodology

The present design studies are focussed on the machine operating in motoring mode as this allows a more consistent approach to be taken in terms of fixing the torque and power specification which lends itself to analytical modelling. More specifically, the torque rating of the machine is not dependent on the machine losses so various designs can be performed for a known fixed torque with losses being supplied from the converter side. Therefore, a fixed power rating of 250 kW is set for each machine in a series of designs.

To provide a representative performance constraint, each machine was designed to provide constant power over a 5:1 speed range though field weakening. The specifics of the designs to realise this level field weakening are not the focus of this paper. The 5:1 speed range is simply used to establish the maximum rated

torque at base speed and the mechanical centrifugal load at the maximum speed. The latter plays a role in determining torque density because of the influence that it has over the thickness of the rotor containment sleeve and hence the effective magnetic air gap of a given design.

For each set of design constraints considered here, a series of machines were designed with a base speed of 1000 rpm, up to a base speed of 14,000 rpm. The corresponding torque specifications and maximum speeds are summarised in Table 1. Surface-mounted permanent magnet machine with concentrated windings were selected as the topology.

In order to undertake a systematic investigation of torque density variation with speed rating, constraints need to be applied onto the design of machines belonging to one series. In this study, three sets of constraints are investigated, namely,

- Constant current density and split ratio
- Constant current density and electric loading (Q)
- Constant heat flux per unit of core back surface area

The detailed specifications for each set of constraints will be demonstrated in later sections, respectively. Besides these highly specific constraints, there are some shared constraints by all the machine series, namely, the slot-pole configuration, the slot packing factor, the aspect ratio etc. In this study, the 9-slot-8-pole configuration is investigated, due to its highest winding factor in the all tooth wound concentrated winding machines, and thus the highest torque output provided the same electric and magnetic loadings. A packing factor, i.e. the proportion of the slot cross-sectional area occupied by coppers was set to 0.5 for all machines considered. Finally, a fixed 1:1 axial length to stator overall diameter aspect ratio was adopted. Since the machine is designed for aerospace applications with high ambient temperature, Sm<sub>2</sub>Co<sub>17</sub>, with remanent flux density 1 T and relative permeability 1.05, was specified. The stator and rotor cores were assumed to be manufactured using Vacoflux 50 Cobalt-Iron.

### 2.1 Constant current density and split ratio design

For this set of design constraints, the current density and the split ratio (i.e. ratio of airgap diameter to overall stator diameter) were kept constant at 10 A/mm<sup>2</sup> and 0.6, respectively. This value of current density is representative of fairly aggressive cooling,

**Table 1** Specifications of the designed machines

Machine number	Rated power, kW	Base rotating speed, rpm	Maximum rotating speed, rpm	Torque required at base speed, Nm
1	250	1000	5000	2387
2		2000	10,000	1194
3		3000	15,000	796
4		4000	20,000	597
5		5000	25,000	477
6		6000	30,000	398
7		7000	35,000	341
8		8000	40,000	298
9		9000	45,000	265
10		10,000	50,000	239
11		12,000	60,000	199
12		14,000	70,000	171

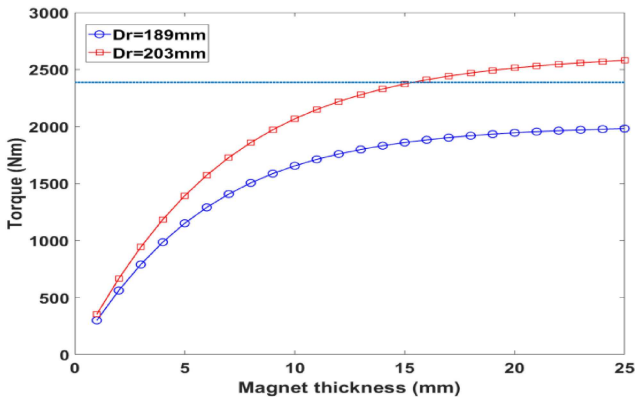


**Fig. 1** Torque variation with magnet thickness (machines 1)

although it is some way short of the 12–15 A/mm<sup>2</sup> that can be considered with direct or spray oil cooling. In sizing each machine in the series, an approach, which combines the benefits of analytical and finite element methods, are used. The sizing of the machine is based on the well-established torque equation:

$$T = \frac{\pi^2}{4\sqrt{2}} k_w B_{ave} Q_{rms} D_r^4 L_a \quad (1)$$

where  $k_w=0.945$  is the winding factor,  $B_{ave}$  is the magnetic loading,  $Q_{rms}$  is the rms electric loading,  $D_r$  is the rotor diameter, and  $L_a$  is the axial length. For a 1:1 machine aspect ratio, namely,  $L_a = (D_r/s)$ , where  $s$  is the split ratio, (1) can be reformulated into

$$T = \frac{\pi^2}{4\sqrt{2}} k_w B_{ave} Q_{rms} \frac{D_r^3}{s} \quad (2)$$

For the particular set of design constraints set in this case, the rms electric loading  $Q_{rms}$  is not constant, but it can be expressed in terms of slot area and the fixed current density, namely,

$$Q_{rms} = \frac{k_p J_{rms} N_s A_{slot}}{\pi D_r} \quad (3)$$

where  $k_p$  is the slot packing factor,  $J_{rms}$  is the rms winding current density,  $N_s$  is the number of stator slots, and  $A_{slot}$  is the slot area. With some manipulation, the expression (3) can be fully expressed in terms of the rotor diameter  $D_r$ . This necessarily requires a consistent means of sizing the stator teeth and back iron which itself requires an estimate of the average air-gap flux density, the design flux density level for the stator core and the tooth pitch to slot pitch ratio. Adopting an air-gap flux density which is 80% of the magnet remanence and specifying a core flux density for sizing purposes of 1.8 T and a tooth pitch to slot pitch ratio of 0.8, it can be shown that:

$$A_{slot} = 0.07 D_r^4 \quad (4)$$

Substituting (3) and (4) back into (2) yields:

$$T = \frac{0.07\pi}{4\sqrt{2}s} k_w k_p B_{ave} J_{rms} N_s D_r^4 \quad (5)$$

Hence

$$D_r^4 = \frac{4\sqrt{2}sT}{0.07\pi k_w k_p B_{ave} J_{rms} N_s} \quad (6)$$

This provides a design value for  $D_r$ , albeit one based on several simplifications, notably assuming that the average flux density that can be achieved is 80% of the remanence. In order to achieve this level of flux density, and hence torque, it is necessary to an appropriate magnet thickness. The selection of a magnet thickness, however, needs to take account of the need for a containment sleeve whose thickness is itself dependant on the magnet thickness.

Recourse to the finite element analysis, albeit only two-dimensional in the first instance, is essential in order to refine the machine design since both inter-polar leakage in the air gap with thick containment sleeves and the onset of magnetic saturation in the stator core at rated load may introduce appreciable errors in the analytical torque estimates. This will inevitably lead to some iteration of the rotor diameter to ensure that the power specification is met. This can be illustrated by considering two specific cases from the 14 design specifications. Starting with the lowest speed design (1000 rpm base speed), the value of  $D_r$  from (6) is 188.8 mm. This value was used in a series of two-dimensional finite element calculations for a range of magnet thicknesses from 1 mm to 25 mm, in each case with a fixed rotor magnet outer diameter of  $D_r$ . In each case, the containment thickness required for the maximum speed (5,000 rpm in this case) was calculated using the analytical mechanical stress model proposed in [5] and a maximum design stress of 1 GPa, a value which is representative of that achievable with a high-performance carbon-fibre composite. Since  $D_r$  remains fixed at 188.8 mm and the split ratio also remains fixed at 0.6, any increase in containment thickness reduces the available space of the stator. At a fixed current density, this will result in a gradual reduction in the electric loading. This containment sleeve thickness when added to the specific mechanical clearance between the rotor and stator of 0.5 mm yields the overall effective magnetic air gap.

Fig. 1 shows the resulting variation in the finite element calculated torque as a function of magnet thickness for the original value of  $D_r$ . As will be apparent, this falls short of the specification of 2387 Nm and hence some increase in  $D_r$  is required, recalling that for a fixed split ratio and aspect ratio, this will result in a proportional increase in the stator outer diameter and axial length. Fig. 1 also shows a corresponding variation in torque with magnet thickness for a revised  $D_r$  of 203 mm calculated using finite element analysis, from which it is apparent that the torque

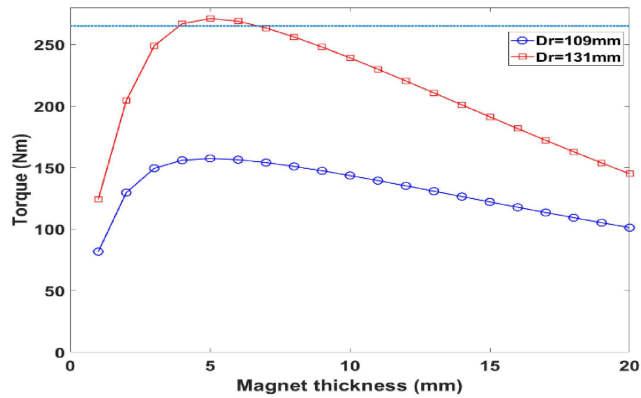


Fig. 2 Torque variation with magnet thickness (machine 9)

Table 2 Key dimensions of constant split ratio (0.6) and constant current density (10 A/mm<sup>2</sup>) series

Machine number	Rotor diameter, mm	Stator outer diameter, mm	Magnet thickness, mm	Containment thickness, mm	Torque, Nm	Power, kW
1	203	338	15	0.50	2376	249
2	170	283	12	0.57	1230	258
3	154	257	10	0.89	814	256
4	145	242	8	1.15	608	255
5	139	232	7	1.49	487	255
6	135	225	6	1.78	404	254
7	133	222	5	2.03	347	255
8	130	217	5	2.61	297	249
9	131	218	4	2.81	267	251
10	134	223	3	2.93	245	256
11	142	237	2	3.85	199	251

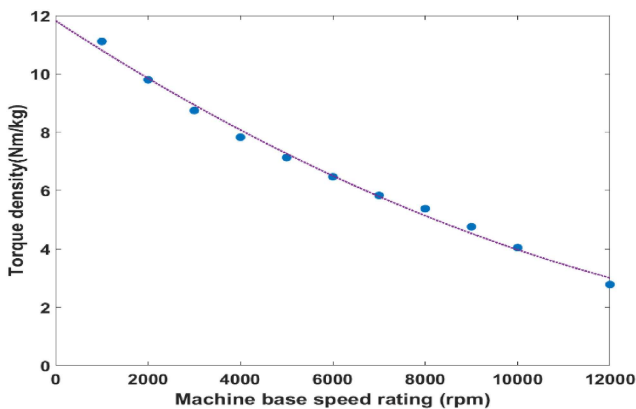


Fig. 3 Torque density variation with base speed for constant split ratio

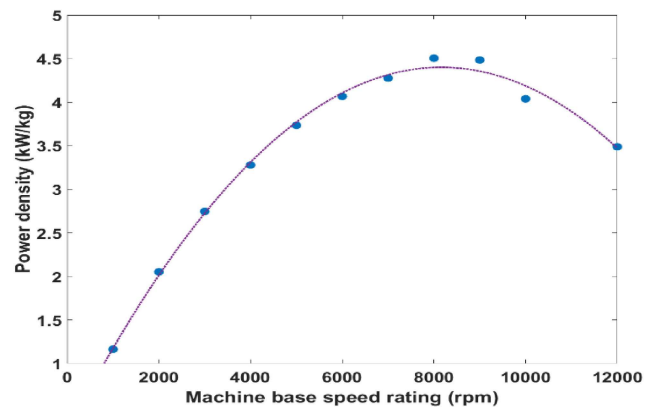


Fig. 4 Power density variation with base speed for constant split ratio

specification can be achieved with a magnet thickness of 15 mm. It is interesting to note that with this combination of magnet and containment sleeve thicknesses (15 and 0.5 mm, respectively), the average air-gap flux density calculated from finite element analysis is 0.68 T. This became the final design of machine 1.

It is also useful to consider in detail design 9, which shows behaviour that is representative of that for the higher base speed designs. In this case, the initial value of  $D_r$  calculated using (6) was 109 mm. The variation in torque with magnet thickness for this value of  $D_r$  is shown in Fig. 2. As will be apparent, in this case, the original value of  $D_r$  falls well short of the torque specification of 265 Nm. Following iterations, a final value of 131 mm was used for  $D_r$ . The resulting variation in torque calculated by finite element analysis with magnet thickness for this revised value of  $D_r$  is also shown in Fig. 2. An interesting feature of the form of the curve in Fig. 2 is the presence of a clear optimum in magnet thickness, i.e. 5 mm in this case. This is a consequence of the influence of the containment sleeve thickness on the effective magnetic air gap outweighing the benefits of increased magnet

thickness. A similar procedure was repeated for the remaining 12 designs, which resulted in the establishment of the series of design detailed in Table 2. In the case of designs with a base speed of 14,000 rpm (design 12), the required power of 250 kW could not be achieved within this set of constraints, the maximum achievable being 203 kW. This shortfall could be overcome by relaxing the constraint on the axial which is limited by the 1:1 aspect ratio constraint imposed. The torque density and power density variations with machine base speed rating for these two series are shown in Figs. 3 and 4, respectively.

As will be apparent from Fig. 3, there is a progressive decrease in torque density as the base speed for the design increases. Eventually, the torque density decreases at a faster rate than the increases in speed, leading to an optimum base speed specification in terms of power density, namely, 8,000 rpm for this particular set of constraints.

The trends observed can be analytically interpreted by deriving the expression for torque density using (1):

$$\text{Torque density} \propto \frac{1}{\delta_{\text{ave}}} B D_r s^2 \quad (7)$$

The average mass density is made up from a combination of core density, magnet density, and copper density (with due account of the coil packing factor). This average mass density will inevitably vary with different proportions of these constituent components. However, for 14 machine designs considered, the variation is small from a maximum of  $7028 \text{ kg m}^{-3}$  to a minimum (at the high base speed end) of  $6906 \text{ kg m}^{-3}$ . Although the value of  $7000 \text{ kg m}^{-3}$  is somewhat specific to a split ratio of 0.6, this potentially has some value more broadly in machine design for simplified mass estimation.

## 2.2 Constant current density and electrical loading design

Further series of designs were established, but in this case with a fixed current density of  $10 \text{ A/mm}^2$  and three discrete levels of electrical loading, namely,  $50 \text{ A/mm}$ ,  $125 \text{ A/mm}$ , and  $200 \text{ A/mm}$ . In these series of designs, the split ratio is not fixed as was the case previously. Starting from (1) shown previously for the torque, in terms of the rotor magnet outer diameter  $D_r$ , the equation can be re-arranged to:

$$D_r^2 = \frac{4\sqrt{2}T}{\pi^2 L_d k_w B_{\text{ave}} Q_{\text{rms}}} \quad (8)$$

Whereas this might appear more straightforward since the electric loading is specified, the expression still contains the axial length. For the imposed constraint of an aspect ratio of 1, the axial length is equivalent to the stator outer diameter. In order to address this difficulty, the sizing (1) is further developed into

$$T = \frac{\pi^2}{4\sqrt{2}} k_w B_{\text{ave}} Q_{\text{rms}} D_r^2 \left[ 2h_{bi} + \frac{N_s}{\pi} w_t + 2\sqrt{\left( R_1 - \frac{N_s}{2\pi} w_t \right)^2 + \frac{N_s}{\pi} A_{\text{slot}}} \right] \quad (9)$$

where  $h_{bi}$  is the stator back-iron thickness,  $w_t$  is the stator tooth width, and the radius  $R_1$  has the following expression

$$R_1 = \sqrt{\left( \sqrt{(R_r + L_g)^2 - (w_t/2)^2} + h_{\text{tip}} \right)^2 + (w_t/2)^2} \quad (10)$$

with  $h_{\text{tip}}$  being the bottom thickness of stator tooth tip. Equation (9) can be used to solve for  $D_r$ , although it should be recognised that several of the terms such as  $w_t$  and  $h_{\text{tip}}$  are linked to  $D_r$  and hence a numerical approach is required. Having established an initial value of  $D_r$ , the same iterative approach using finite element analysis was used to arrive at the series of designs for each of the three specified levels of electric loading.

The torque density and power density variation with speed rating for constant electric loading and constant current density designs are shown in Fig. 5 and 6, respectively. As will be apparent, for this new set of constraints, there are many more designs which are not capable of meeting the power specification, especially at low electric loading, where machines usually have large diameters to meet the torque specifications, and thus big containment thickness. This illustrates the critical role that the mechanical properties of the containment sleeve have on power density. As was the case with the constraint of a fixed split ratio and stator current density, there is a marked reduction in torque density with the base speed of design, and again an optimum base speed in terms of power density is achieved.

## 2.3 Constant heat flux per unit of core back surface area

Ultimately, it is usually thermal considerations that limit power density in electrical machines. Whereas the constant current density constraints considered above provide a reasonable proxy of constant loss density in the winding, they do not consider the full thermal consequences of speed increases. In the final series of

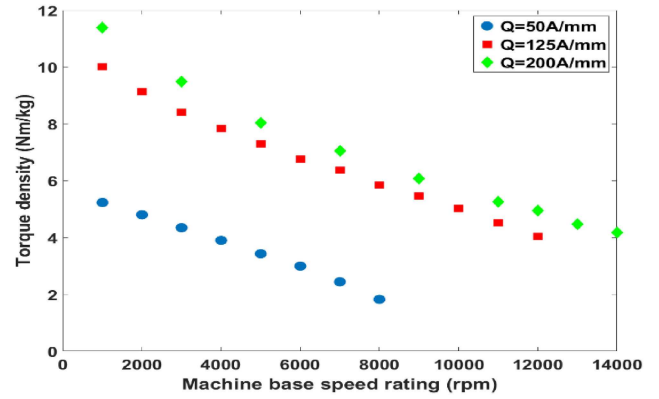


Fig. 5 Torque density variation with machine speed rating (constant electric loading design)

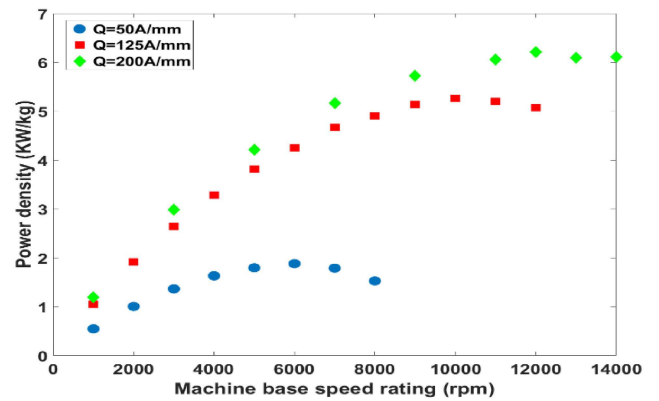


Fig. 6 Power density variation with machine speed rating (constant electric loading design)

designs, the copper and iron loss for each design operating at its load point was calculated and the design dimensions iterated until the total loss per unit of core back surface area converged on one of two prescribed values of  $24.6 \text{ kW/m}^2$  and  $15 \text{ kW/m}^2$ . The former is the value achieved with the very first design considered here, i.e.  $1,000 \text{ rpm}$  base speed design with a split ratio of 0.6 and a rms current density of  $10 \text{ A/mm}^2$ . In this design, only copper loss and iron loss were considered as heat sources. Parasitic losses, such as AC winding loss, rotor magnet loss, and mechanical losses like friction loss, are not considered.

In each case, the copper loss was calculated on the basis of room temperature resistance and the core losses at the rated operating point using a finite element simulation over one electrical cycle in combination with an element-by-element application of a time-domain loss separation model of the type described in [6]. The material-specific constants adopted were those for Vacoflux 50 cobalt iron from [7]. Table 3 summarises the resulting designs, while Fig. 7 and 8 show the resulting variation in torque and power density.

## 2.4 Effect of aspect ratio on torque density and power density variation

The effect of aspect ratio on torque density and power density variation was investigated, specifically in terms of establishing a further series of design to the same specification but with a length to diameter aspect ratio of 2:1 for a fixed constant split ratio of 0.6 and a fixed rms current density of  $10 \text{ A/mm}^2$  (i.e. the same design constraints as those used in section 2.1). The same combined analytical and finite element method were used for machine sizing, and refinement and the magnet thickness was optimised in the same manner.

As indicated from (2), the output torque is linearly proportional to axial length  $L_a$ , but proportional to the cube of rotor diameter. Due to the fact that the machine volume is proportional to square of the product of the stator outer diameter and axial length, then for

**Table 3** Key parameters of the machine series with constant heat flux per unit surface area

Machine base speed rating, rpm	Electrical rotor diameter, mm	Stator outer diameter, mm	Stator tooth height, mm	Current density, A/mm <sup>2</sup>	Split ratio	Axial length, mm
heat flux = 24.6 kW/m <sup>2</sup> .						
1000	203	338	44	10	0.60	338
2000	170	273	31	12	0.62	283
3000	154	244	27	13	0.63	257
4000	145	229	24	13	0.63	242
5000	139	220	23	13	0.63	232
6000	135	214	22	13	0.63	225
7000	133	212	22	13	0.63	222
8000	130	207	21	13	0.63	217
9000	131	212	23	12	0.62	218
10,000	134	228	29	9	0.59	223
heat flux = 15 kW/m <sup>2</sup> .						
1000	203	368	59	7	0.55	338
2000	170	301	46	8	0.56	283
3000	154	271	40	8	0.57	257
4000	145	256	38	8	0.57	242
5000	139	248	37	7	0.56	232
6000	135	245	38	7	0.55	225
7000	133	251	42	6	0.53	222
8000	130	250	42	5	0.52	217

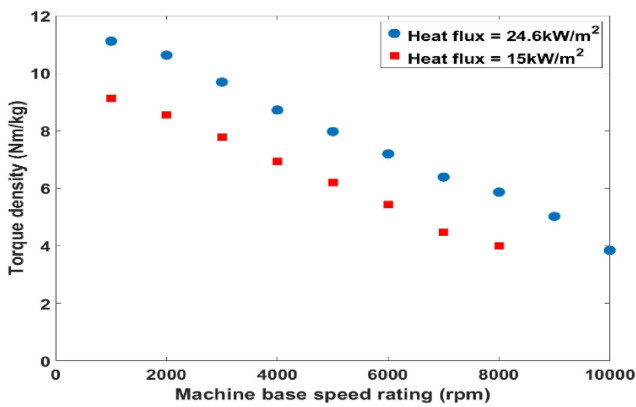


**Fig. 7** Torque density variation with machine speed rating (constant heat flux per unit core back surface area)

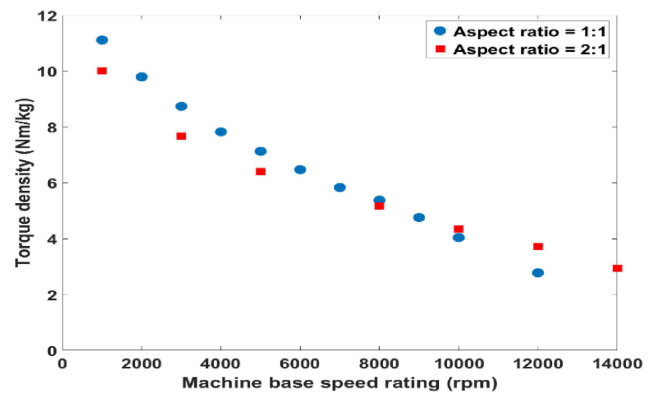


**Fig. 9** Torque density variation with machine speed rating (different aspect ratio)

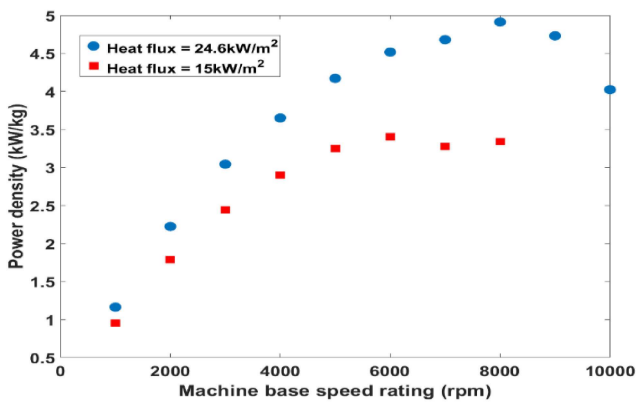


**Fig. 8** Power density variation with machine speed rating (constant heat flux per unit core back surface area)

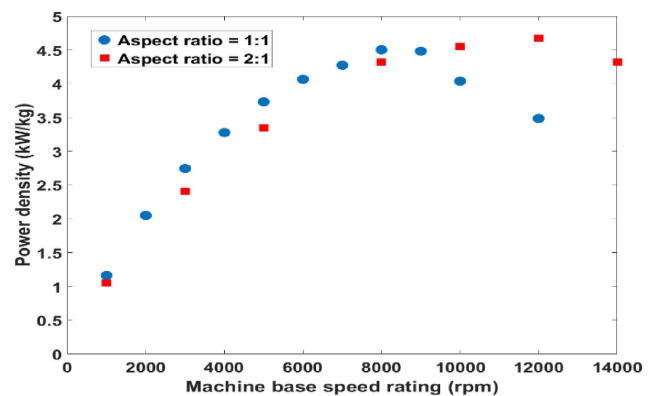


**Fig. 10** Power density variation with machine speed rating (different aspect ratio)

a constant split ratio design criteria, doubling the axial length cannot achieve an equal return in terms of a reduction in machine volume under the same torque output requirement, and inevitably the overall machine size would increase when changing the aspect ratio from 1:1 to 2:1. This qualitative discussion is supported by the behaviour exhibited in Figs. 9 and 10 at the low speed end where the machine series with 2:1 aspect ratio has lower torque

density and power density than a corresponding machine with a 1:1 aspect ratio. However, at the high speed end, where the effect of containment thickness comes strongly into play, the benefit of having smaller rotor diameter for machine series with 2:1 aspect ratio starts to yield dividends. Above certain speed rating, the torque density and power density of a machine design with 2:1 aspect ratio are greater than its counterpart with a 1:1 aspect ratio. As also shown, the 2:1 aspect ratio is able to yield viable designs

that meet the 250 kW power rating criterion across the full range of base speeds considered, while the 1:1 designs as discussed previously fall short on power at the 14,000 rpm base speed design point.

### 3 Conclusion

Several series of machines have been designed and analysed to investigate the influence on torque density and power density of machine speed rating. It has been demonstrated that the various degrees to which torque density decreases with speed rating, due to a complex interaction between electromagnetic and mechanical considerations. Indeed, for some combinations of power/speed ratings and design constraints, there may well be an optimum speed in terms of power density, beyond which the power density starts to decrease. Finally, it is worth concluding that this study is rather specific to the power and speed ranges considered and care should be taken in applying the trends in torque density to very different specifications, in particular those in which mechanical considerations due to a combination of large diameter and high speed are not as pronounced. In these cases, the well-established maxim that power will always increase with speed will hold up rather better than was the case in this study.

### 4 Acknowledgments

The authors acknowledge the financial and technical support provided by Rolls-Royce to this project.

### 5 References

- [1] Boglietti, A., Cavagnino, A., Tenconi, A., *et al.*: 'Key design aspects of electrical machines for high-speed spindle applications'. IECON 2010 - 36th Annual Conf. on IEEE Industrial Electronics Society, Glendale, AZ, USA, 2010, pp. 1735–1740
- [2] Arkkio, A., Jokinen, T., Lantto, E.: 'Induction and permanent-magnet synchronous machines for high-speed applications'. Proc. of the Eighth Int. Conf. on Electrical Machines and Systems, 2005 (ICEMS 2005), Nanjing, China, 2005, vol. 2, pp. 871–876
- [3] Zwyssig, C., Kolar, J., Round, S.D.: 'Mega-speed drive systems: pushing beyond 1 million r/min', *IEEE/ASME Trans. Mechatronics*, 2009, **14**, (5), pp. 564–574
- [4] Kolondzovski, Z., Arkkio, A., Larjola, J., *et al.*: 'Power limits of high-speed permanent-magnet electrical machines for compressor applications', *IEEE Trans. Energy Convers.*, 2011, **26**, pp. 73–82
- [5] Harris, C.O.: 'Introduction to stress analysis' (The MacMillan company, New York, 1959), p. 256
- [6] Atallah, K., Howe, D.: 'The calculation of iron losses in brushless permanent magnet dc motors', *J. Magn. Magn. Mater.*, 1994, **133**, pp. 578–582
- [7] Rodrigues, L.K., Jewell, G.W.: 'Model specific characterization of soft magnetic materials for core loss prediction in electrical machines', *IEEE Trans. Magn.*, 2014, **50**, (11), pp. 1–4
- [8] EL-Refaie, A.M.: 'Fractional-Slot concentrated-windings synchronous permanent magnet machines: opportunities and challenges', *IEEE Trans. Ind. Electron.*, 2010, **57**, (1), pp. 107–121
- [9] Hendershot, J.R.Jr., Miller, T.J.E.: 'Design of brushless permanent-magnet motors' (Oxford, 1994)